

## Supporting Information

# Ultrathin flexible reduced graphene oxide /cellulose nanofiber composite films with strongly anisotropic thermal conductivity and efficient electromagnetic interference shielding

*Weixing Yang, Zedong Zhao, Kai Wu, Rui Huang, Tianyu Liu, Hong Jiang, Feng*

*Chen\* and Qiang Fu\**

College of Polymer Science and Engineering, State Key Laboratory of Polymer

Materials Engineering, Sichuan University, Chengdu 610065, China.

### Corresponding author

E-mail: qiangfu@scu.edu.cn (Q. Fu), Tel./Fax: +86- 28-8546 1795.

E-mail: fengchen@scu.edu.cn (F. Chen), Tel./Fax: +86-28-85460690.

### **Preparation of cellulose nanofibers (CNFs).**

The microfibrillated cellulose (2 g) was first dispersed in deionized water (400 ml) containing TEMPO (0.032 g) and sodium bromide (0.2 g). The oxidation reaction was started by adding the desired amount of the NaClO solution (10 mmol per gram of MFC) dropwise into the dispersion at room temperature under continuous stirring. During the oxidation process, the pH was maintained at 10 by adding 0.5 M NaOH using a pH stat until no decrease in pH was observed. The TEMPO-oxidized cellulose was thoroughly washed with deionized water by filtration until the filtrated solution was neutral. After the treatment, approximately 0.3 wt% TEMPO-oxidized cellulose suspension was sonicated for 15 min at power of 300 W in an ice bath. Cellulose nanofibers dispersion was achieved by centrifugation at 10000 rpm for 10 min to remove the unfibrillated cellulose. The cellulose nanofibers dispersion was stored at 4°C before used.

### **Preparation of graphene oxide (GO) nanosheets.**

Firstly, graphite (2 g) and NaNO<sub>3</sub> (1 g) were mixed together and cooled to 0 °C. H<sub>2</sub>SO<sub>4</sub> (98 %, 50 ml) was added to the mixture and stirred uniformly, then KMnO<sub>4</sub> (6 g) was slowly added over 1h. The reaction temperature was kept at 0 °C for 2 h. After removal of the ice-bath, the reaction was heated to 35 °C and stirred for 30 min. Deionized water (100 ml) was added slowly to the mixture while maintaining the reaction temperature at 98 °C for 3h. The mixture was then allowed to cool, 5 % H<sub>2</sub>O<sub>2</sub> (50 ml) was added to the mixture with continuous stirring at room temperature. The color of the mixed solution changed to golden yellow. The graphite oxide was washed and centrifuged with deionized water repeatedly to remove residual salts and acids. To exfoliate graphitic oxide into graphene oxide, the mixture was treated with ultrasonication for 30 min.

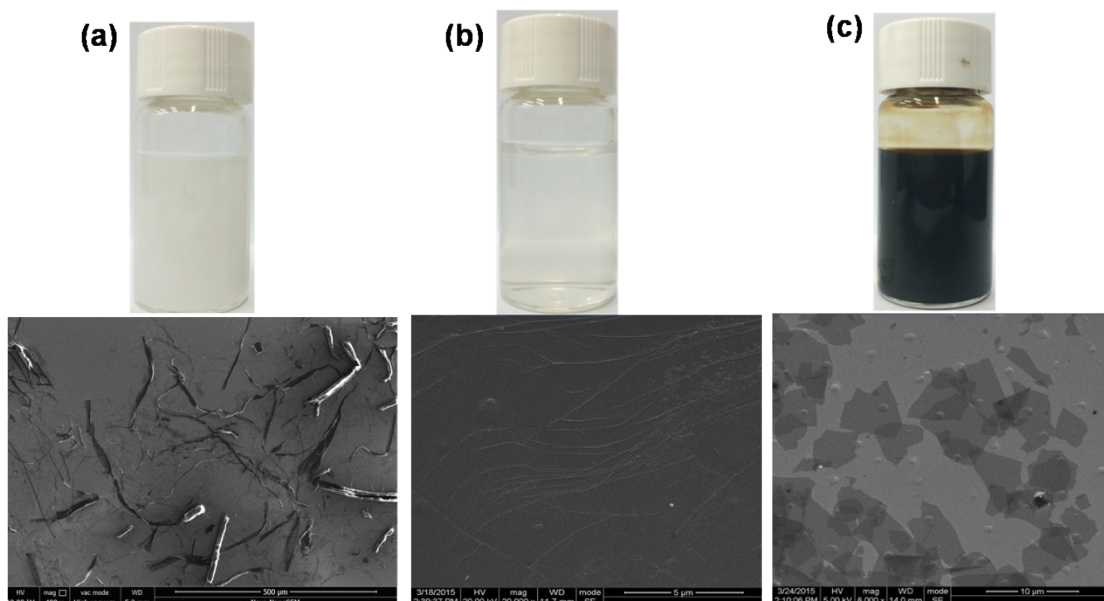


**Fig. S1** SEM images of original microfibrillated cellulose (a), cellulose nanofiber (b) and graphene oxide nanosheets (c).

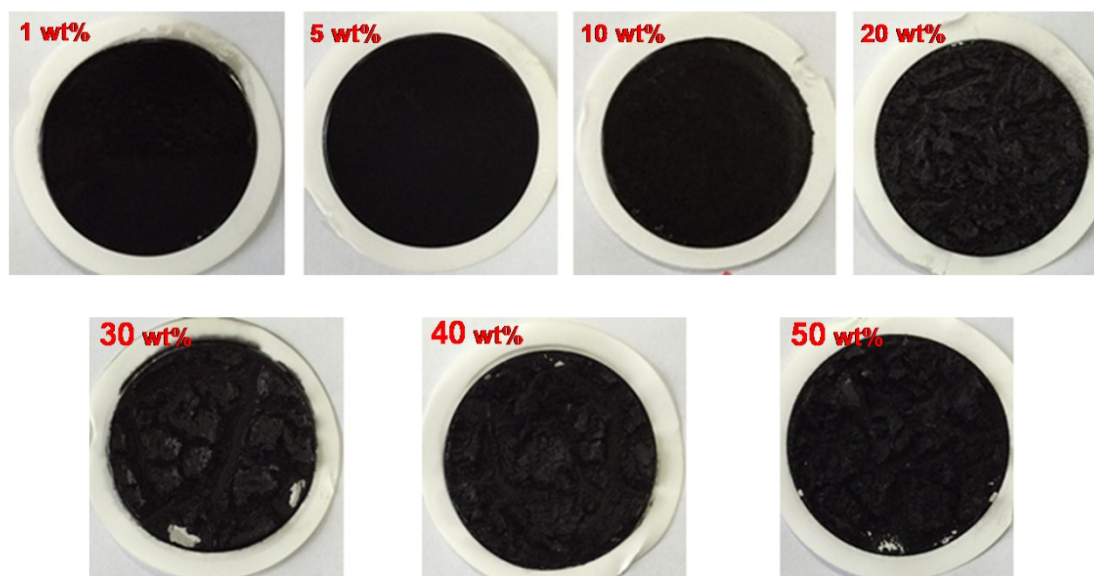


**Fig. S2** Photographs of RGO/CNF composite films with different RGO contents of 1 wt%, 5 wt%, 10 wt%, 20 wt%, 30 wt%, 40 wt%, and 50 wt%, which were made by filtering reduced graphene oxide/CNF emulsions.

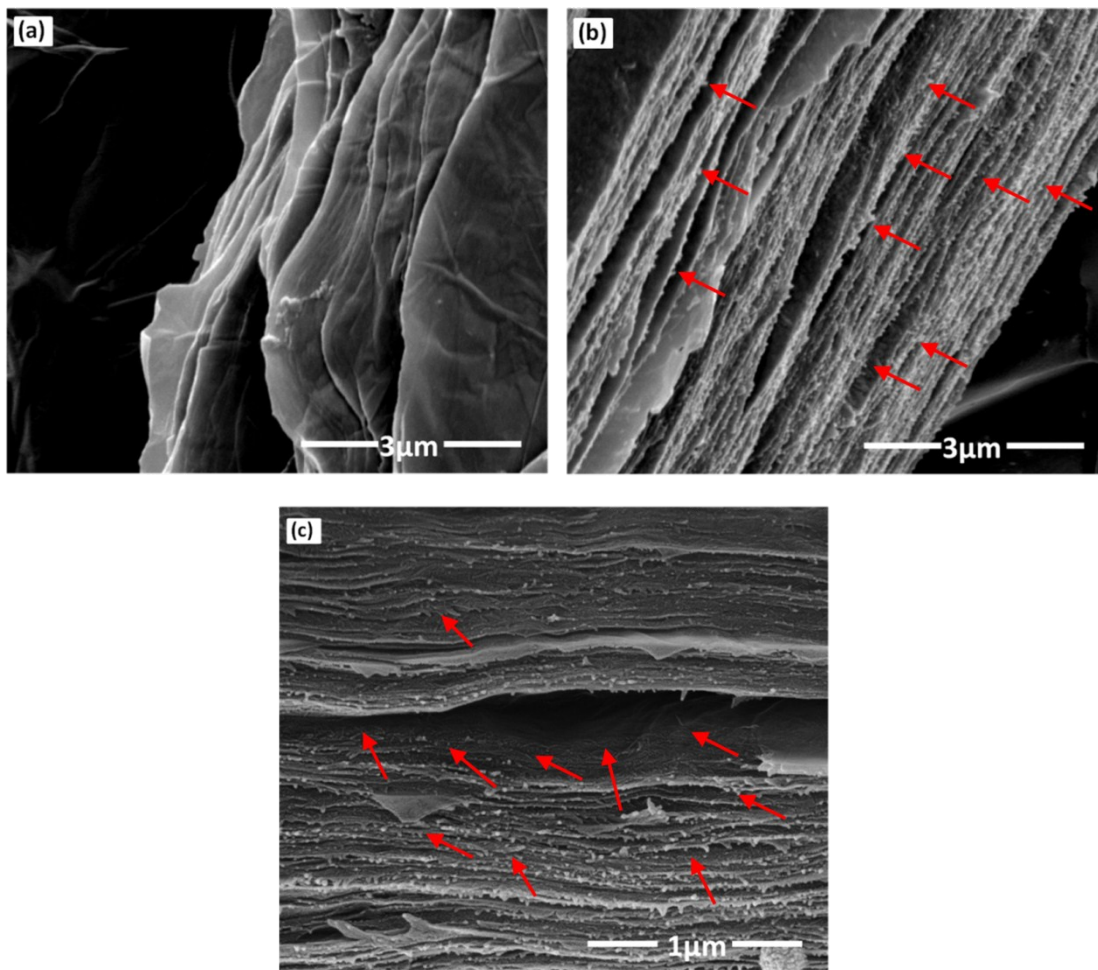


**Fig. S3** Scanning electron microscopy images of fracture surfaces of RGO film (a) and CNF/RGO-50 composite film (b, c). The arrow points to cellulose nanofiber.

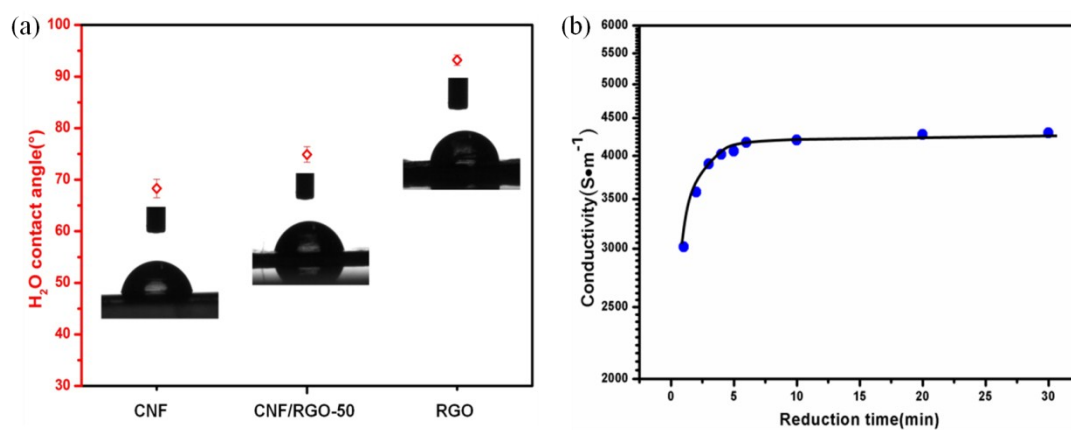


**Fig. S4** Photographs showing the water contact angle of CNF film, CNF/RGO-50 and RGO film (a), and variation of electrical conductivity of the CNF/GO-50 films with time as a result of 45% HI acid reduction at 80°C (b).

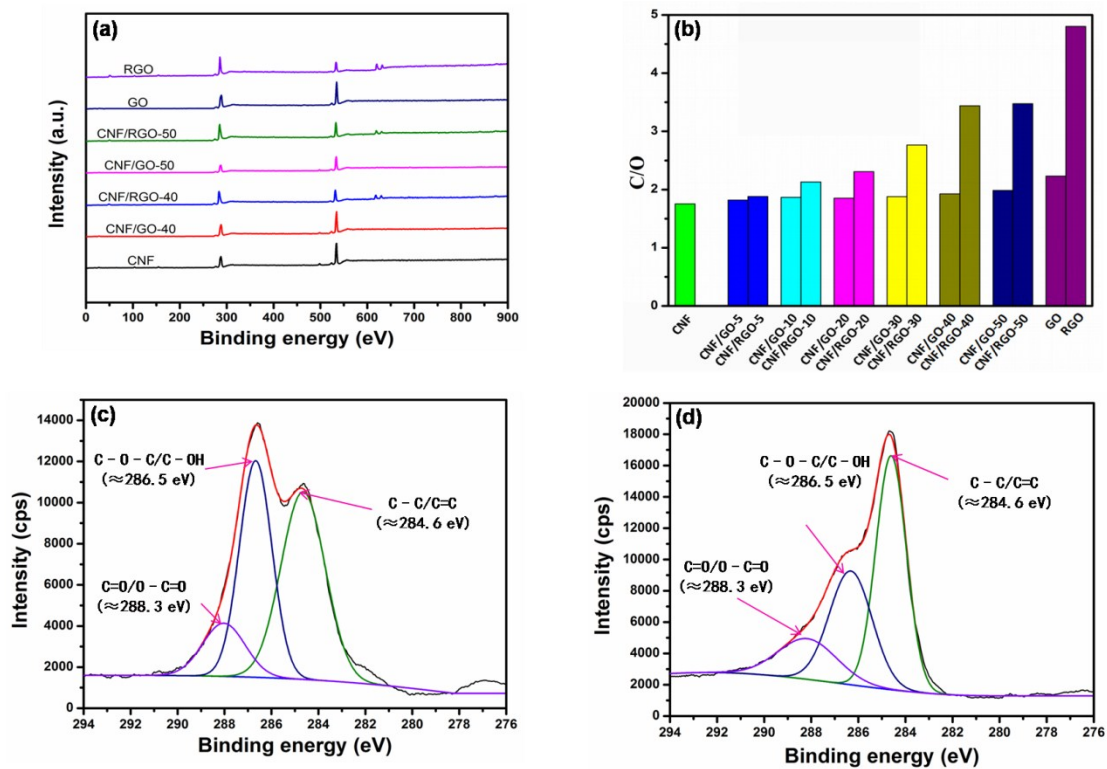


**Fig. S5** (a, b) XPS spectra and variation of the C/O atomic ratio of the neat CNF film and hybrid films of before and after reduction by hydroiodic acids. (c, d) X-ray photoelectron spectroscopy data of the carbon signatures for (c) CNF/GO-40 composite film and (d) CNF/RGO-40 composite film.

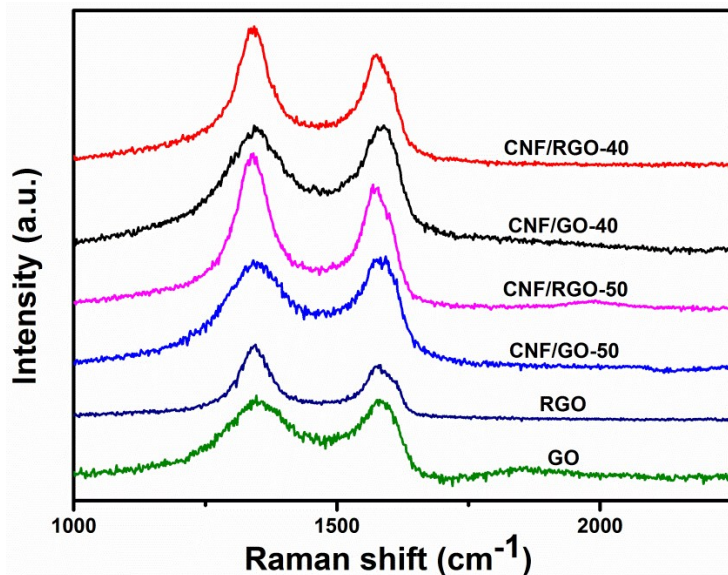


**Fig. S6.** Raman spectra of GO, RGO, CNF/GO-50, CNF/RGO-50, CNF/GO-40 and CNF/RGO-40 films with a laser of 532 nm.

**Tab. S1** EMI SE of carbon-based polymer composites in the X-band frequency range

Materials	Thickness (mm)	Concentration	EMI SE (dB)	Ref
MWCNT/PC	1.15	(0.5-5) wt%	0-20	1
MWCNT/Cellulose	2.5	(1-10) wt%	8.2-22.5	2
MWCNT/WPU	0.05	(0-76.2) wt%	0-24	3
MWCNT/PP	0.34	(1-11.4) vol%	1-22	4
	2.8	(1-5) vol%	2-24	4
MWCNT/PS	2	(1-20) wt%	5-60	5
MWCNT/PTT	2	(0-4.76) vol%	1-22	6
MWCNT/ABS	1.1	(0.5-15) wt%	9-50	7
MWCNT/WPU	1	(0-76.2)wt%	0-21.1	8
Foam				
CB/ABS	1.1	(2.5-15) wt%	2-22	7
CB/EPDM	5.5	(9-37.5) wt%	1-18	9
SWCNT/epoxy	2	(0.01-15)wt%	2-25	10
SWCNT/PU	2	(0-20) wt%	1-17	11
Graphene/WPU	2	(0.1-5) wt%	3-32	12
Graphene/PMMA	3.4	(0-4.23) vol%	0-30	13
Graphene/PS	2.8	(0-15) wt%	0-24	14
Graphene /PEI	2.3	(1-10) wt%	5-20	15
Graphene /PEI	2.3	(1-10) wt%	3-12.8	15
Foam				
Graphene/PS foam	2.5	30 wt%	29	16
Graphene@Fe <sub>3</sub> O <sub>4</sub> / PEI Foam	2.5	(1-10) wt%	3.5-18.2	17
Graphene /PDMS Foam	1	(0-0.8) wt%	0-19.98	18
Graphene/PMMA Foam	2.4	(0-1.8) vol%	0-19	19
Graphene/CNF (this work)	0.023	(0-50) wt%	0-25	

PC, WPU, PP, PS, PTT, ABS, EPDM, PU, PMMA, PEI, PDMS and CNF are polycarbonate, waterborne polyurethane, polypropylene, polystyrene, poly (trimethylene terephthalate), acrylonitrile butadiene styrene copolymers, ethylene propylene diene monomer, polyurethane, poly (methyl methacrylate), polyetherimide, polydimethylsiloxane, cellulose nanofiber, respectively.

**Calculation of EMI shielding effectiveness ( $SE_T$ ), microwave reflection ( $SE_R$ ) and microwave absorption ( $SE_A$ ) from scattering parameters.**

The samples were placed between two X-band waveguide parts that were connected to separate ports of the Agilent N5230 vector network analyzer. From the measured scattering parameters ( $S_{11}$  and  $S_{12}$ ), the power coefficients of reflection (R), transmission (T), and absorption (A) can be obtained, and their relationship is described as  $R+A+T=1$ .<sup>7</sup> The EMI SE values of RGO/CNF composite films ( $SE_T$ ),  $SE_R$ , and  $SE_A$  can then be respectively calculated as follows:

$$SE_T = -10\log T \quad (1)$$

$$SE_R = -10\log(1-R) \quad (2)$$

$$SE_A = SE_T - SE_R - SE_M \quad (3)$$

Where  $SE_M$  is the microwave multiple internal reflections, which can be negligible when  $SE_T \geq 15$  dB.

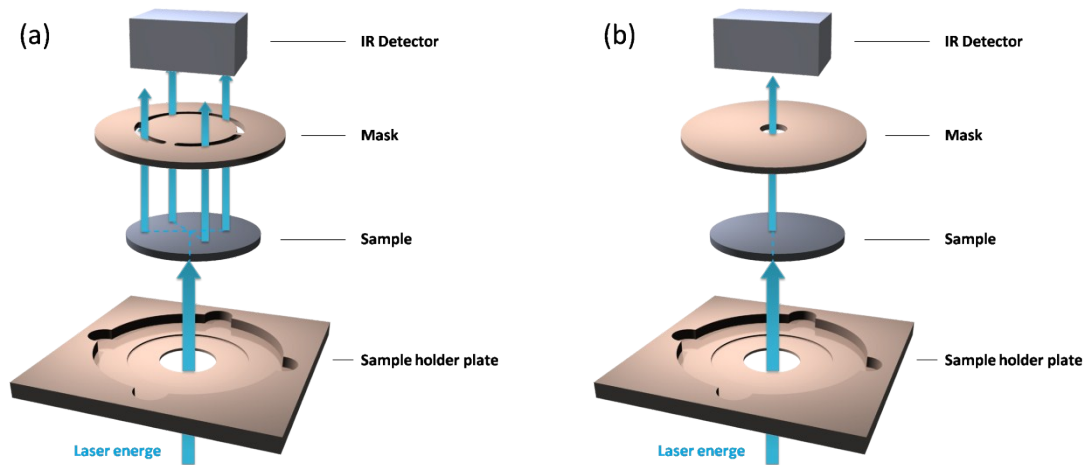


**Fig. S7** Schematic of thermal conductivity measurement setup of in-plane thermal conductivity (a) and the cross-plan thermal conductivity (b).

**Tab. S2** Tensile properties of pure CNF film and RGO/CNF composite films.

RGO Content (wt%)	Tensile strength (MPa)	Young's modulus (GPa)	Elongation (%)
0 (CNF Film)	189.4± 4.5	6342.3± 255.1	7.5± 0.6
5	156.5± 4.4	6533.6± 115.7	3.9± 0.3
10	137.3± 2.9	6698.8± 220.1	2.9±0.2
20	98.1± 3.1	7047.3± 397.1	1.9± 0.1
30	92.9± 2.9	7342.3±262.8	1.7± 0.1
40	85.7± 5.1	7441.0± 121.5	1.6± 0.1
50	67.7± 2.9	7737.9± 77.5	1.4± 0.2
100	17.2±1.1	982.0±44.1	2.3±0.1

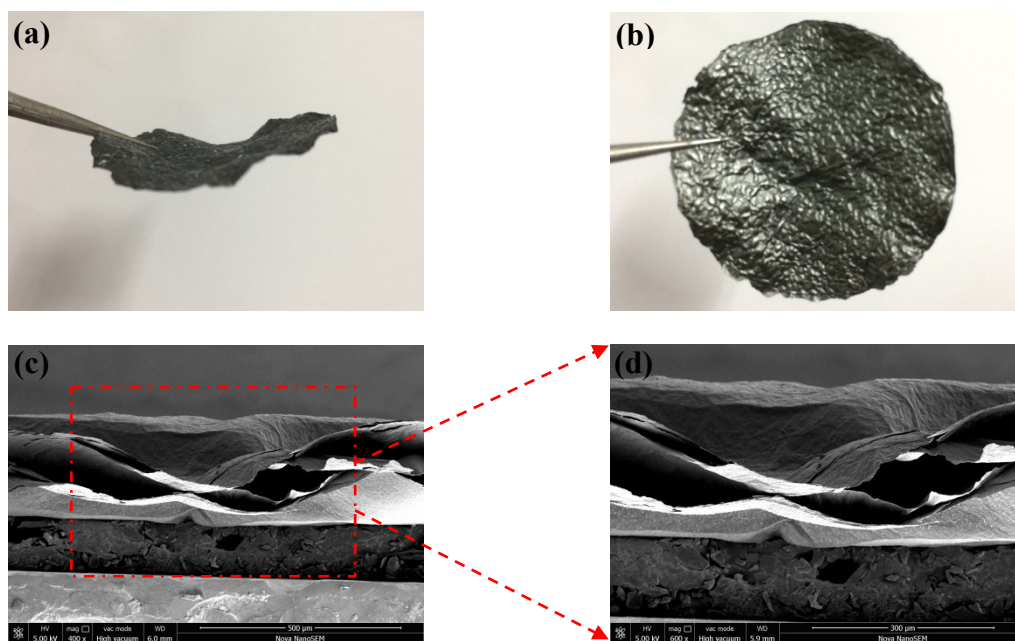


**Fig. S8** Photographs the surface of RGO film (a,b) and SEM images of fracture surface of RGO film(c,d).

## ■ REFERENCES

1. M. Arjmand, M. Mahmoodi, G. A. Gelves, S. Park and U. Sundararaj, *Carbon*, 2011, **49**, 3430-3440.
2. H.-D. Huang, C.-Y. Liu, D. Zhou, X. Jiang, G.-J. Zhong, D.-X. Yan and Z.-M. Li, *J. Mater. Chem. A*, 2015, **3**, 4983-4991.
3. Z. Zeng, M. Chen, H. Jin, W. Li, X. Xue, L. Zhou, Y. Pei, H. Zhang and Z. Zhang, *Carbon*, 2016, **96**, 768-777.
4. M. H. Al-Saleh and U. Sundararaj, *Carbon*, 2009, **47**, 1738-1746.
5. M. Arjmand, T. Apperley, M. Okoniewski and U. Sundararaj, *Carbon*, 2012, **50**, 5126-5134.
6. A. Gupta and V. Choudhary, *J. Mater. Sci.*, 2011, **46**, 6416-6423.
7. M. H. Al-Saleh, W. H. Saadeh and U. Sundararaj, *Carbon*, 2013, **60**, 146-156.
8. Z. Zeng, H. Jin, M. Chen, W. Li, L. Zhou and Z. Zhang, *Adv. Funct. Mater.*, 2016, **26**, 303-310.
9. P. Ghosh and A. Chakrabarti, *Eur. Polym. J.*, 2000, **36**, 1043-1054.
10. Y. Huang, N. Li, Y. Ma, F. Du, F. Li, X. He, X. Lin, H. Gao and Y. Chen, *Carbon*, 2007, **45**, 1614-1621.
11. Z. Liu, G. Bai, Y. Huang, Y. Ma, F. Du, F. Li, T. Guo and Y. Chen, *Carbon*, 2007, **45**, 821-827.
12. S.-T. Hsiao, C.-C. M. Ma, H.-W. Tien, W.-H. Liao, Y.-S. Wang, S.-M. Li and Y.-C. Huang, *Carbon*, 2013, **60**, 57-66.
13. H.-B. Zhang, W.-G. Zheng, Q. Yan, Z.-G. Jiang and Z.-Z. Yu, *Carbon*, 2012, **50**, 5117-5125.
14. C. Li, G. Yang, H. Deng, K. Wang, Q. Zhang, F. Chen and Q. Fu, *Polym. Int.*, 2013, **62**, 1077-1084.
15. J. Ling, W. Zhai, W. Feng, B. Shen, J. Zhang and W. g. Zheng, *ACS Appl. Mater. Interfaces*, 2013, **5**, 2677-2684.
16. D.-X. Yan, P.-G. Ren, H. Pang, Q. Fu, M.-B. Yang and Z.-M. Li, *J. Mater. Chem.*, 2012, **22**, 18772-18774.
17. B. Shen, W. Zhai, M. Tao, J. Ling and W. Zheng, *ACS Appl. Mater. Interfaces*, 2013, **5**, 11383-11391.
18. Z. Chen, C. Xu, C. Ma, W. Ren and H.-M. Cheng, *Adv. Mater.*, 2013, **25**, 1296-1300.
19. H.-B. Zhang, Q. Yan, W.-G. Zheng, Z. He and Z.-Z. Yu, *ACS Appl. Mater. Interfaces*, 2011, **3**, 918-924.